ATMOSPHERIC AND OCEANIC SCIENCE LETTERS, 2014, VOL. 7, NO. 5, 447–452

The Combined Effect of Initial Error and Model Error on ENSO Prediction Uncertainty Generated by the Zebiak-Cane Model

ZHAO Peng[1,2] and DUAN Wan-Suo[1*]

[1] *State Key Laboratory of Numerical Modeling for Atmospheric Sciences and Geophysical Fluid Dynamics (LASG), Institute of Atmospheric Physics, Chinese Academy of Sciences, Beijing 100029, China*
[2] *University of Chinese Academy of Sciences, Beijing 100049, China*

Received 25 March 2014; revised 20 April 2014; accepted 22 April 2014; published 16 September 2014

Abstract Initial errors and model errors are the source of prediction errors. In this study, the authors compute the conditional nonlinear optimal perturbation (CNOP)-type initial errors and nonlinear forcing singular vector (NFSV)-type tendency errors of the Zebiak-Cane model with respect to El Niño events and analyze their combined effect on the prediction errors for El Niño events. The CNOP-type initial error (NFSV-type tendency error) represents the initial errors (model errors) that have the largest effect on prediction uncertainties for El Niño events under the perfect model (perfect initial conditions) scenario. However, when the CNOP-type initial errors and the NFSV-type tendency errors are simultaneously considered in the model, the prediction errors caused by them are not amplified as the authors expected. Specifically, the prediction errors caused by the combined mode of CNOP-type initial errors and NFSV-type tendency errors are a little larger than those caused by the NFSV-type tendency errors. This fact emphasizes a need to investigate the optimal combined mode of initial errors and tendency errors that cause the largest prediction error for El Niño events.

Keywords: predictability, initial error, model error, optimal perturbation

Citation: Zhao, P., and W.-S. Duan, 2014: The combined effect of initial error and model error on ENSO prediction uncertainty generated by the Zebiak-Cane model, *Atmos. Oceanic Sci. Lett.*, **7**, 447–452, doi:10.3878/j.issn.1674-2834.14.0034.

1 Introduction

The El Niño-Southern Oscillation (ENSO) is the most prominent climate phenomenon of interannual variability. Successful and accurate predictions of ENSO are extremely important for human society and economies. Although great progress has been made in recent decades in forecasting ENSO, significant prediction errors still exist, and the results of prediction are unsatisfactory (Jin et al., 2008).

Generally, the uncertainty of prediction comes from two aspects: initial errors and model errors. Many studies have explored the effect of initial errors on ENSO predictability and emphasized the important role of initial errors in a successful ENSO forecast, ultimately concluding that initial errors may have a great effect on ENSO prediction (Samelson and Tziperman, 2001; Mu et al., 2007). Mu et al. (2003) proposed conditional nonlinear optimal perturbation (CNOP), which is an extension of the linear singular vector (LSV) (Lorenz, 1965) to nonlinear fields, to represent the initial errors that cause the largest prediction errors in nonlinear models. Also, some studies have demonstrated the roles played by model errors in yielding significant prediction errors (Blanke et al., 1997; Latif et al., 1998; Williams, 2005; Zheng et al., 2006; 2009). Model errors consist of the combined effect of uncertainties of unrecognized physical processes (Syu and Neelin, 2000), sub-grid parameterization, and atmospheric noises, or other high-frequency variations such as westerly wind bursts and the Madden-Julian oscillation (Gebbie et al., 2007; Marshall et al., 2009). Duan and Zhou (2013) proposed the Nonlinear Forcing Singular Vector (NFSV), which represents the tendency error that induces the largest prediction errors. Base on this approach, Duan and Zhao (2014)[①] used the Zebiak-Cane model to study the effect of tendency errors on prediction uncertainties of ENSO.

In realistic ENSO predictions, both initial errors and model errors exist simultaneously. Consequently, it is necessary to consider the combined effect of these errors on the uncertainty of ENSO forecasts. In this context, we ask: How does the combined mode of CNOP and NFSV influence the ENSO prediction error? Is it the optimal combined mode of initial error and tendency error that causes the largest prediction error? We address these two questions in the present paper by using the CNOP and NFSV approaches.

2 Conditional nonlinear optimal perturbation and the nonlinear forcing singular vector

The CNOP is an initial perturbation that satisfies a given constraint and has the largest nonlinear evolution at the prediction time (Mu et al., 2003). For an appropriate measurement, $\|\ \|$, the initial perturbation, $\boldsymbol{w}_{0\delta}$, can be defined as CNOP if and only if it satisfies

$$J(\boldsymbol{w}_{0\delta}) = \max_{\|\boldsymbol{w}_0\|_a \leqslant \delta_1} \left\| \boldsymbol{M}_{t_0,t_k}(\boldsymbol{W}_0 + \boldsymbol{w}_0) - \boldsymbol{M}_{t_0,t_k}(\boldsymbol{W}_0) \right\|_b, \quad (1)$$

*Corresponding author: DUAN Wan-Suo, duanws@lasg.iap.ac.cn

[①] Duan, W. S., and P. Zhao, 2014: Revealing the most disturbing tendency error of Zebiak-Cane model associated with El Niño predictions by nonlinear forcing singular vector approach, *Climate Dyn.*, in revison.

where $\| \ \|_a$ and $\| \ \|_b$ are selected according to specific physical problems, and used to measure the amplitudes of initial errors, $\boldsymbol{w}_0$, and the prediction errors induced by $\boldsymbol{w}_0$, respectively. δ_1 is the constraint radius of $\boldsymbol{w}_{0\delta}$, and $\boldsymbol{M}_{t_0,t_k}$ is the propagator of a nonlinear model from time t_0 to t_k. $\boldsymbol{W}_0$ is the initial value of the basic state, and $\boldsymbol{w}_0$ is its initial perturbation. The CNOP represents the initial errors that have the largest effect on prediction errors.

The NFSV is a tendency perturbation that satisfies a given constraint and has the largest nonlinear evolution at the prediction time (Duan and Zhou, 2013). The NFSV, $\boldsymbol{f}_\delta$, can be defined by presenting a constrained maximization problem:

$$J(\boldsymbol{f}_\delta) = \max_{\|\boldsymbol{f}\|_a \leqslant \delta_2} \left\| \boldsymbol{M}_{t_0,t_k}(\boldsymbol{f})(\boldsymbol{W}_0) - \boldsymbol{M}_{t_0,t_k}(0)(\boldsymbol{W}_0) \right\|_b , \quad (2)$$

where $\boldsymbol{M}_{t_0,t_k}(\boldsymbol{f})$ is the propagator of the nonlinear model with tendency equation superimposed tendency error, $\boldsymbol{f}$; $\| \ \|_a$ and $\| \ \|_b$ are used to measure the amplitude of tendency errors, $\boldsymbol{f}$, and the prediction error induced by $\boldsymbol{f}$; δ_2 is the constraint radius of $\boldsymbol{f}$. From Duan and Zhou (2013), the NFSV describes the tendency error that causes the largest prediction error.

3 CNOP-type initial errors and NFSV-type tendency errors of El Niño events in the Zebiak-Cane model

The Zebiak-Cane model (Zebiak and Cane, 1987) was the first coupled ocean-atmosphere model to successfully simulate ENSO interannual variability. It has been widely used in ENSO prediction and predictability research owing to its good performance (Zebiak and Cane, 1987; Blumenthal, 1991; Mu et al., 2007; Duan et al., 2012; Yu et al., 2012), and can be regarded as a platform for investigating the combined effect of initial errors and tendency errors on the predictability of ENSO.

Two groups of model El Niño events are selected as the reference-state El Niño events to be predicted, including four weak El Niño events (denoted by W1–W4), and four strong El Niño events (denoted by S1–S4) (see Fig. 1).

To obtain CNOPs and NFSVs of the reference-state El Niño events, we use $\| T'(t_k) \|_a = \sqrt{\sum_{i,j} (T'_{i,j}(t_k))^2}$ to measure the prediction errors caused by initial errors, $\boldsymbol{w}_0$, or tendency errors, $\boldsymbol{f}$, at prediction time t_k; $T'_{i,j}(t_k)$ represents the prediction errors of the SST anomalies (SSTA) at the grid (i, j) caused by $\boldsymbol{w}_0$ or $\boldsymbol{f}$ at prediction time t_k. The grid (i, j) is in the domain of the tropical Pacific, with latitude from 19°S to 19°N by 2°, and longitude from 129.375°E to 84.375°W by 5.625°. Next, we construct the corresponding cost function according to Eqs. (1) and (2):

$$J(\boldsymbol{w}_{0\delta_1}) = \max_{\|\boldsymbol{w}_0\| \leqslant \delta_1} \| T'(t_k) \|_a , \quad (3)$$

$$J(\boldsymbol{f}_{\delta_2}) = \max_{\|\boldsymbol{f}\| \leqslant \delta_2} \| T'(t_k) \|_a , \quad (4)$$

where the constraint bounds, δ_1 of CNOP and δ_2 of NFSV, are experimentally predetermined as 0.8 and 0.4, respectively.

We use Year(0) to represent the year when El Niño attains a peak value, Year(−1) and Year(1) to denote the year before and after Year(0), respectively. For each El Niño, we make predictions for 12 months with the start month of July(−1) (i.e., July in Year(−1)), October(−1), January(0), April(0), July(0), October(0), January(1), and April(1). For each start month, the El Niño is predicted by using the Zebiak-Cane model with the CNOP-type initial error and the NFSV-type tendency error, respectively. Therefore, each El Niño event will have 16 predictions with eight start months and a total of 128 predictions are made for the eight El Niño events.

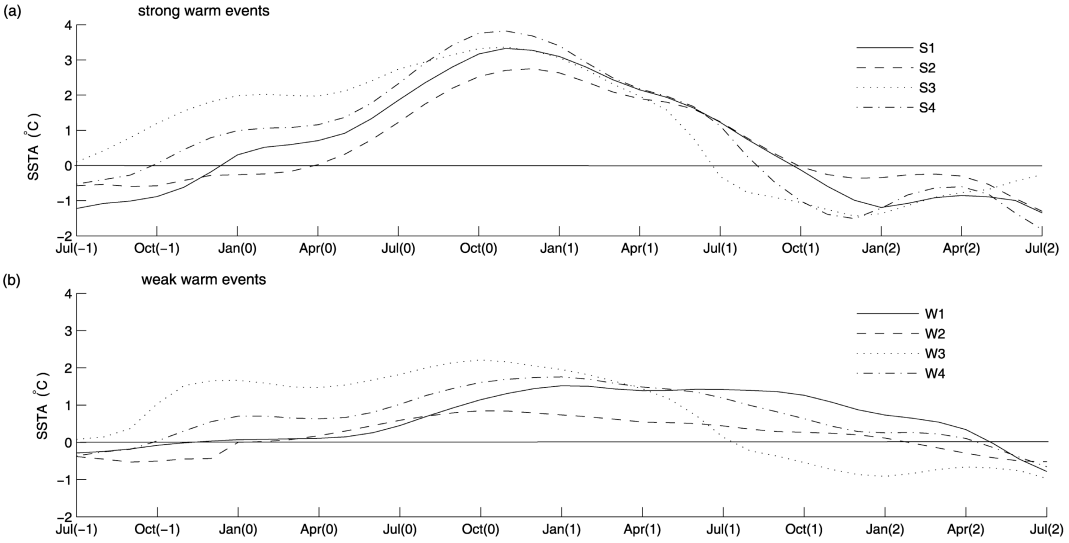

Figure 1 (a) The Niño-3 indexes of four strong El Niño events, denoted by S1–S4, and (b) those of four weak El Niño events, denoted by W1–W4.

By solving Eqs. (3) and (4), we can obtain 64 CNOPs and 64 NFSVs, respectively. By analyzing the CNOPs and NFSVs, we find that they are independent of the intensities of the El Niño events, but dependent on start months. According to the start months, the CNOPs (Fig. 2; also see Yu et al. (2009)) and the NFSVs (Fig. 3; also see Duan and Zhao (2014)[①]) can be classified into two types, respectively. When the predictions are initialized in July(−1), October(−1), January(0), and April(0), the CNOP-type initial errors tend to be of the SSTA component with positive anomalies in the eastern Pacific and negative anomalies in the central-western Pacific, and of the thermocline depth anomaly component with a deepening along the equator (for simplicity, we call this type of initial errors "type-1 CNOP" initial errors). We note that the predictions with the start months July(−1), October(−1), January(0), and April(0) often cross the growth phase of the El Niño events. Therefore, the predictions through the growth phase of El Niño are inclined to possess type-1 CNOP initial errors. However, when the predictions start

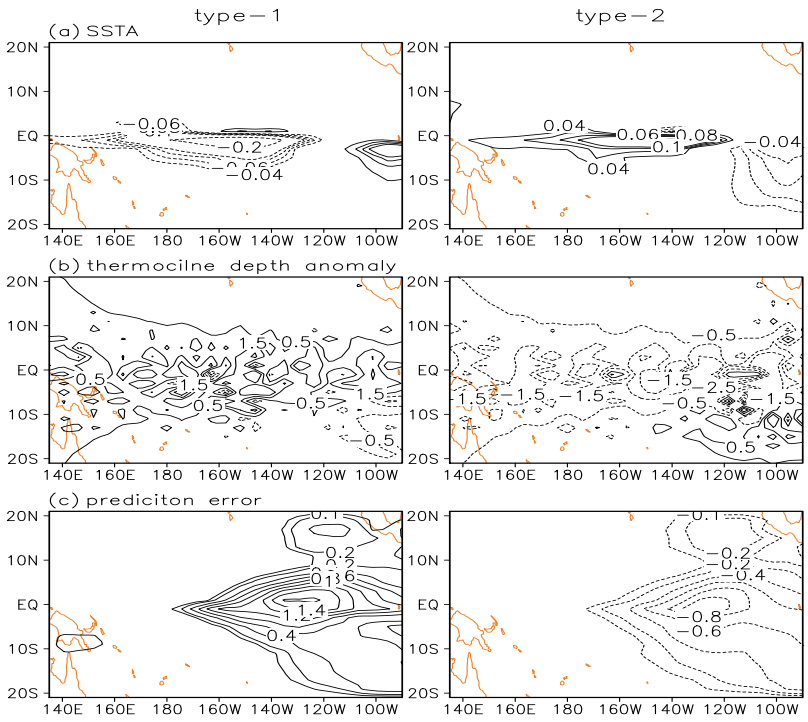

Figure 2 Two types of the conditional nonlinear optimal perturbation (CNOP)-type initial errors and resultant prediction errors with a lead time of 12 months. The CNOP consists of (a) SSTA and (b) thermocline depth anomaly components, and (c) the prediction errors are for SSTA. The left column shows type-1 CNOP initial error, and the right column shows type-2 CNOP initial error. The type-1 and -2 CNOPs are calculated with the initial time of January(0) and January(1) for the El Niño denoted by S1.

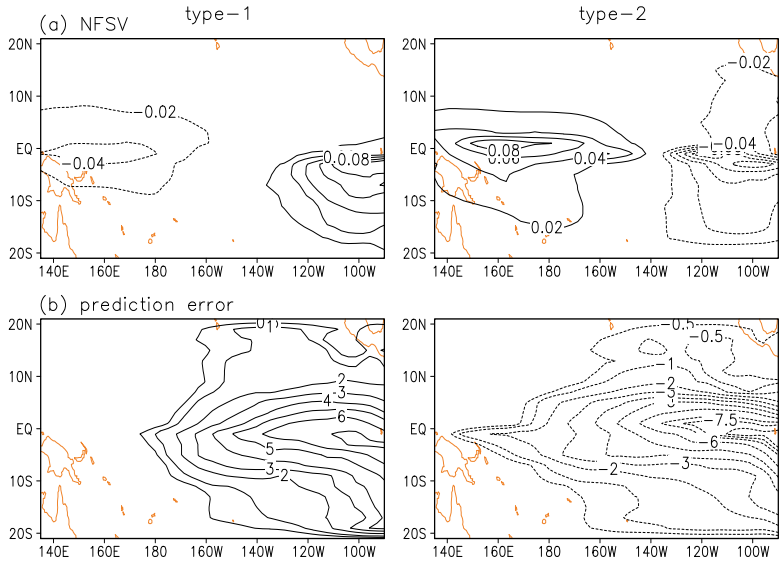

Figure 3 Two types of NFSV-type (a) tendency errors and (b) the resultant prediction errors with a lead time of 12 months. The left column shows type-1 NFSV tendency error, and the right column shows type-2 tendency error. The type-1 and -2 NFSVs consist of the SSTA component and are calculated with the initial time of January(0) and January(1) for the reference-state El Niño denoted by S1.

in July(0), October(0), January(1), and April(1), and through the decaying phase of El Niño, the CNOP-type initial errors tend to be of SSTA and thermocline depth anomaly patterns almost opposite to the type-1 CNOP initial errors. We similarly call this type of initial errors "type-2 CNOP" initial errors.

The NSFV-type tendency errors consist of the SSTA component. From Fig. 3, it is clearly shown that the two types of NFSVs are very similar to the SSTA components of the CNOP-type initial errors, which are similarly denoted by "type-1 NFSV" and "type-2 NFSV". However, it should be pointed out that the type-1 NFSV tendency errors are related to the predictions associated with the decaying phase of El Niño, while the type-2 NFSV tendency errors are related to the predictions of the growth phase. In any case, we notice that both the CNOP-type initial errors and the NFSV-type tendency errors possess the same regions of large errors. The similarities between CNOP and NFSV indicate that the El Niño predictions may be sensitive to not only initial errors but also the tendency errors in these regions.

4 The combined effect of CNOP-type initial errors and NFSV-type tendency errors on El Niño prediction uncertainties

In this section, we investigate the effect of the combined mode of CNOP-type initial errors and NFSV-type tendency errors on prediction errors of El Niño events. We superimpose CNOP-type initial error and NFSV-type tendency error on the initial state of the reference-state El Niño events and the SST-tendency equation and integrate the perturbed model for 12 months, obtaining predictions for the reference-state El Niño events influenced by the CNOP-type initial errors and NSFV-type tendency errors. By subtracting the reference-state El Niño events from their predictions, the prediction errors induced by the combined mode of CNOP-type initial errors and NFSV-type tendency errors can be obtained. As a comparison, we also calculate the CNOP- and NFSV-resultant prediction errors.

In Fig. 4, we plot a histogram of the ensemble mean of the prediction errors caused by CNOP-type initial errors, NFSV-type tendency errors, and their combined mode for strong El Niño events. By comparing the results, we find that the NFSV-type tendency errors tend to cause a slightly larger prediction error than the combined mode of CNOP-type initial errors and NFSV-type tendency errors. For weak El Niño events, we also obtain similar results. However, these results are not as we expected, i.e., that the combined mode of CNOP-type initial errors and NFSV-type tendency errors would cause a much larger prediction error than the NFSV-type tendency errors because much more uncertainty are considered in the model by including initial errors and tendency errors. So, what is the reason for this result?

To address this question, we examine the patterns of CNOP-type initial errors and NFSV-type tendency errors reported in the last section. As revealed in section 3, the CNOP-type initial errors tend to be type-1 errors in the predictions associated with the growth phase of El Niño events, but type-2 errors in the predictions of the decaying phase. The type-1 CNOP initial errors often evolve into an El Niño-like mode and cause El Niño events to be overpredicted; while the type-2 CNOP initial errors develop into a La Niña-like mode and cause El Niño to be underpredicted (see Fig. 2c and Yu et al. (2009)). However, for the NFSV-type tendency errors, although the type-1 (type-2) NFSV tendency errors have similar patterns to the type-1 (type-2) CNOP initial errors, they occur in the predictions associated with the decaying (growth) phase of El Niño. That is to say, the predictions associated with the growth (decaying) phase of El Niño tend to be significantly influenced by the type-1 (type-2) CNOP initial errors and the type-2 (type-1) NFSV tendency errors. From Fig. 3, it is shown that the type-1 NFSV tendency errors, similar to the type-1 CNOP type initial errors, tend to present an El Niño-like evolving mode and cause El Niño to be overpredicted; while the type-2 NFSV tendency errors are inclined to show a La Niña-like evolving mode and cause El Niño events to be underpredicted. Therefore, for the type-1 CNOP initial errors and type-2

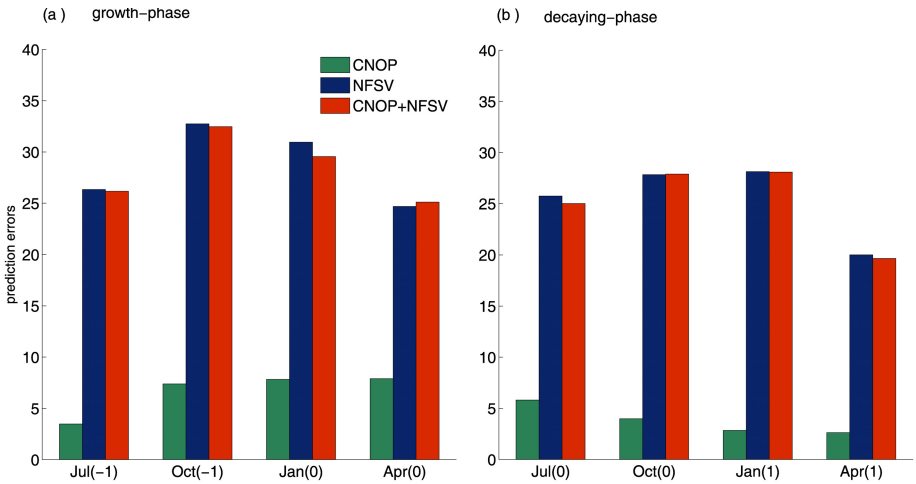

Figure 4 The Ensemble mean of prediction errors caused by CNOP-type initial errors (green bars), NFSV-type tendency errors (blue bars), and their combined mode (red bars) for the strong events (S1–S4) shown in Fig. 1. Panel (a) is the growth-phase prediction and (b) is the decaying-phase prediction. The months on the horizontal axis are the start months of the predictions.

NFSV tendency errors occurring in the predictions associated with the growth phase of El Niño, the prediction errors caused by the type-2 NFSV tendency errors will be counteracted by the prediction errors caused by the type-1 CNOP initial errors, ultimately causing the prediction errors induced by the combined mode of CNOP and NFSV to be smaller than those induced by the type-2 NFSV tendency errors. Similarly, the decaying-phase prediction errors caused by the type-1 NFSV tendency errors will be counteracted by the prediction errors caused by the type-2 CNOP initial errors and cause the prediction errors induced by the combined mode of CNOP and NFSV to be smaller than those induced by the type-1 NFSV tendency errors.

From Fig. 4 we notice that, although the prediction errors caused by the combined mode of CNOP-type initial errors and NFSV-type tendency errors are smaller than those caused by the NFSV-type tendency errors, the differences between the former and the latter are not equal to the prediction errors caused by the CNOP-type initial errors. This indicates that nonlinear interaction exists between CNOP-type initial errors and NFSV-type tendency errors when they are simultaneously present in the model. That is to say, a simple combination of CNOP and NFSV may not mean a straightforward overlapping of the prediction errors that they cause, which sheds light on the fact that the prediction errors caused by the combined modes of CNOP-type initial errors and NFSV-type tendency errors are not larger than those caused by the NFSV-type tendency errors only. Therefore, a simple combination of CNOP and NFSV may not be the optimal combined mode of initial errors and tendency errors, which encourages us to explore in future work the combined mode of initial errors and tendency errors that have the largest effect on prediction errors.

5 Summary and discussion

Within the framework of the Zebiak-Cane model, CNOP and NFSV approaches are used to investigate the combined effect of initial errors and model errors on prediction uncertainty. We calculate the CNOP-type initial errors and NFSV-type model errors of 128 predictions for eight El Niño events with different start months. The results indicate that the prediction errors caused by the combined modes of CNOP- and NFSV-type errors are larger than the resultant prediction error of CNOP-type initial errors, but are not larger than the NFSV-type tendency errors in most situations. In fact, the CNOPs and NFSVs can be classified into two types denoted by type-1 and type-2, respectively. The type-1 NFSVs and CNOPs have similar patterns as positive anomalies in the equatorial eastern Pacific and negative anomalies in the equatorial central-western Pacific. However, the type-2 NFSVs and CNOPs, although they are similar, have signs almost opposite to the type-1 CNOPs and NFSVs. Predictions crossing the growth phase of El Niño are inclined to possess type-1 CNOP-type initial error and type-2 NFSV-type tendency error, which results in the prediction errors caused by NFSV being offset by those caused by CNOP, ultimately inducing their combined mode to cause a smaller prediction error, even when compared to that caused by the NFSV-type tendency error. However, predictions crossing the decaying phase of El Niño tend to possess type-2 CNOPs and type-1 NFSVs. Similarly, the prediction errors caused by their combined mode may induce a smaller prediction error than the NFSVs.

We attempt in the present paper to estimate the largest prediction error caused by initial errors and tendency errors. According to the results, the combined mode of the CNOP-type initial error and the NFSV-type tendency error may not cause a larger prediction error than the NFSV-type tendency errors, and may therefore not be the optimal combined mode of initial errors and tendency errors that causes the larges prediction error. Therefore, in future work it is necessary to explore the optimal combined mode of initial error and tendency error and identify useful information for improving the forecast skill. Moreover, we should establish a cost function to measure the prediction errors caused by the combined mode of initial errors and model errors and explore the optimal combined mode of initial errors and model errors that cause the largest prediction uncertainty.

Acknowledgements. The authors greatly appreciate the anonymous reviewers for their very useful comments and suggestions. This work was jointly sponsored by the National Basic Research Program of China (Grant No. 2012CB955202), the National Public Benefit (Meteorology) Research Foundation of China (Grant No. GYHY201306018), and the National Natural Science Foundation of China (Grant Nos. 41176013 and 41230420).

References

Blanke, B., J. D. Neelin, and D. Gutzler, 1997: Estimating the effect of stochastic wind stress forcing on ENSO irregularity, *J. Climate*, **10**(7), 1473–1486.

Blumenthal, M. B., 1991: Predictability of a coupled ocean-atmosphere model, *J. Climate*, **4**(8), 766–784.

Duan, W. S., and F. F. Zhou, 2013: Non-linear forcing singular vector of a two-dimensional quasi-geostrophic model, *Tellus A*, **65**, doi:10.3402/Tellusa.V65i0.18452.

Duan, W. S., Y. S. Yu, H. Xu, et al., 2012: Behaviors of nonlinearities modulating the El Niño events induced by optimal precursory disturbances, *Climate Dyn.*, **40**(5–6), 1399–1413.

Gebbie, G., I. Eisenman, A. Wittenberg, et al., 2007: Modulation of westerly wind bursts by sea surface temperature: A semistochastic feedback for ENSO, *J. Atmos. Sci.*, **64**(9), 3281–3295.

Jin, E. K., L. James, B. Wang, et al., 2008: Current status of ENSO prediction skill in coupled ocean-atmosphere models, *Climate Dyn.*, **31**(6), 647–664.

Latif, M., D. Anderson, T. Barnett, et al., 1998: A review of the predictability and prediction of ENSO, *J. Geophys. Res.*, **103**(C7), 14375–14393.

Lorenz, E. N., 1965: A study of the predictability of a 28-variable atmospheric model, *Tellus*, **17**, 321–333.

Marshall, A. G., O. Alves, and H. H. Hendon, 2009: A coupled GCM analysis of MJO activity at the onset of El Niño, *J. Atmos. Sci.*, **66**(4), 966–983.

Mu, M., W. S. Duan, and B. Wang, 2003: Conditional nonlinear optimal perturbation and its applications, *Nonlinear Proc. Geophys.*, **10**, 493–501.

Mu, M., H. Xu, and W. S. Duan, 2007: Season-dependent dynamics

of nonlinear optimal error growth and El Niño-Southern Oscillation predictability in a theoretical model, *J. Geophys. Res.*, **112**, D10113, doi:10.1029/2005JD006981.

Samelson, R. M., and E. Tziperman 2001: Instability of the chaotic ENSO: The growth-phase predictability barrier, *J. Atmos. Sci.*, **58**(23), 3613–3625.

Syu, H. H., and J. D. Neelin, 2000: ENSO in a hybrid coupled model. Part I: Sensitivity to physical parametrizations, *Climate Dyn.*, **16**(1), 19–34.

Williams, P. D., 2005: Modelling climate change: The role of unresolved processes, *Philos. Trans. R. Soc. A.*, **363**(1837), 2931–2946.

Yu, Y. Y., W. S. Duan, H. Xu, et al., 2009: Dynamics of nonlinear error growth and season-dependent predictability of El Niño events in the Zebiak-Cane model, *Quart. J. Roy. Meteor. Soc.*, **135**(645), 2146–2160.

Yu, Y. Y., M. Mu, and W. S. Duan, 2012: Does model parameter error cause a significant "Spring Predictability Barrier" for El Niño events in the Zebiak-Cane Model? *J. Climate*, **25**(4), 1263–1277.

Zebiak, S. E., and A. Cane, 1987: A model El Niño-Southern oscillation, *Mon. Wea. Rev.*, **115**, 2262–2278.

Zheng, F., J. Zhu, R. H. Zhang, et al., 2006: Ensemble hindcasts of SST anomalies in the tropical Pacific using an intermediate coupled model, *Geophys. Res. Lett.*, **33**(19), doi:10.1029/2006GL-026994.

Zheng, F., J. Zhu, H. Wang, et al., 2009: Ensemble hindcasts of ENSO events over the past 120 years using a large number of ensembles, *Adv. Atmos. Sci.*, **26**(2), 359–372.